

Resonance and Stellarator Design

Roscoe White
Vinicius Duarte
Andres Bierwage
Stefane Ethier
Kunihiro Ogawa

Princeton 2023

Outline

Motivation

ORBIT simulations

Resonance

Islands with no mode present

Ripple Trapping with no mode present

Chaotic loss due to Alfvén Modes

Conclusion

Main Results

- Resonances of high energy particles in magnetic confinement devices can strongly modify the particle distribution.
Resonance location depends on helicity of the particle orbit, which is energy dependent due to drifts.
- If a resonance matches the period of the equilibrium then:
 1. Islands appear in particle orbits, increasing in size with energy
 2. Local minima produce particle loss due to ripple well trapping.
- A resonance always provides a site for an Alfvén mode.
Mode is likely unstable if there exist local high energy gradients.
- If there is toroidal dependence of B or $\partial B/\partial\psi$ an Alfvén mode produces chaotic loss of particles independent of energy or pitch.

Hamiltonian Guiding Center Code

The covariant expression for the magnetic field used in the guiding center code Orbit is

$$\vec{B} = g(\psi)\nabla\zeta + I(\psi)\nabla\theta + \delta(\psi, \theta, \zeta)\nabla\psi,$$

θ and ζ are poloidal and toroidal coordinates and ψ is the toroidal flux. $g(\psi)$ is the total poloidal current outside the surface ψ , including the current in the field coils.

$I(\psi)$ is the total toroidal plasma current inside ψ .

The Hamiltonian is $H = \rho_{\parallel}^2 B^2 / 2 + \mu B + \Phi$

with $\rho_{\parallel} = v_{\parallel} / B$. Alfvén mode $\delta\vec{B} = \nabla \times \alpha\vec{B}$

Lagrangian with an Alfvén mode present

$$L = (\psi + \rho_{\parallel}I + \alpha I)\dot{\theta} + (\rho_{\parallel}g + \alpha g - \psi_p)\dot{\zeta} + \mu\dot{\xi} - H(\psi_p, \rho_{\parallel}, \theta, \zeta),$$

Resonance

For resonance a particle orbit must periodically return to experience the same perturbation.

Thus, at some time T

$$\theta(T) - \theta(0) = 2\pi p, \quad \zeta(T) - \zeta(0) = 2\pi l, \quad \psi(T) = \psi(0),$$

for integers p, l . The frequency is $\omega = 2\pi/T$,

Launch passing particles distributed in $E, \mu, \psi, \zeta, \theta = 0, \pi$

Poloidal transits $p = \text{mod}(\theta(t) - \theta(0), 2\pi)$

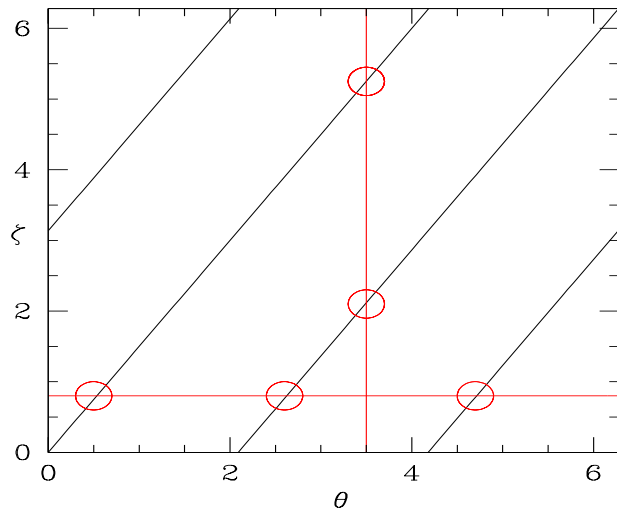
and toroidal transits $l = \text{mod}(\zeta(t) - \zeta(0), 2\pi)$ when orbit returns

Helicity l/p is equal to field line helicity q at low energy

Drift causes resonance to move in minor radius with energy change

Resonance can enter or leave the plasma

3/2 Resonance



Trajectory of a 3/2 resonant particle through multiple transits. Three elliptic points found in any Poincaré section in θ . Two elliptic points found in any Poincaré section in ζ . Normally it is the ζ dependence of an equilibrium that can match the resonance.

Particle Drift

The particle motion in ψ is only drift motion, second order in ρ_{\parallel}

$$\dot{\psi} = -\frac{g}{D}(\mu + \rho_{\parallel}^2 B) \frac{\partial B}{\partial \theta}.$$

The particle motion in the poloidal and toroidal directions are

$$\begin{aligned}\dot{\theta} &= \frac{\rho_{\parallel} B^2}{D}(1 - \rho_{\parallel} g') + \frac{g}{D}(\mu + \rho_{\parallel}^2 B) \frac{\partial B}{\partial \psi_p} \\ \dot{\zeta} &= \frac{\rho_{\parallel} B^2}{D}(q + \rho_{\parallel} I'_{\psi_p}) - \frac{I}{D}(\mu + \rho_{\parallel}^2 B) \frac{\partial B}{\partial \psi_p}.\end{aligned}$$

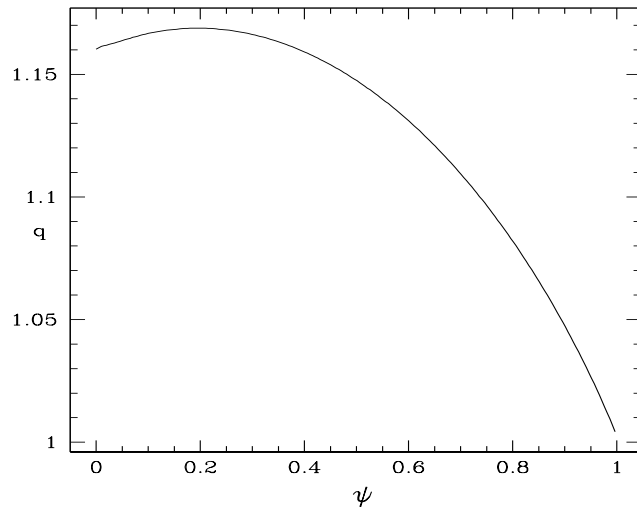
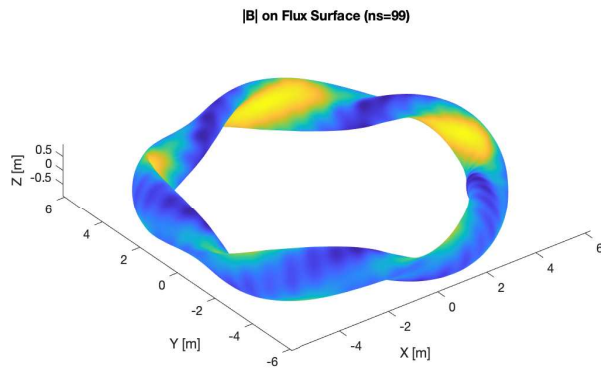
where $D = gq + I + \rho_{\parallel}(gI'_{\psi_p} - Ig'_{\psi_p})$.

At low energy (first order in ρ_{\parallel}) orbit helicity $\dot{\zeta}/\dot{\theta} = q(\psi)$

As the particle energy increases orbit helicity

can either increase or decrease due to drift depending on the orbit.

W7X



Wendelstein 7-X .

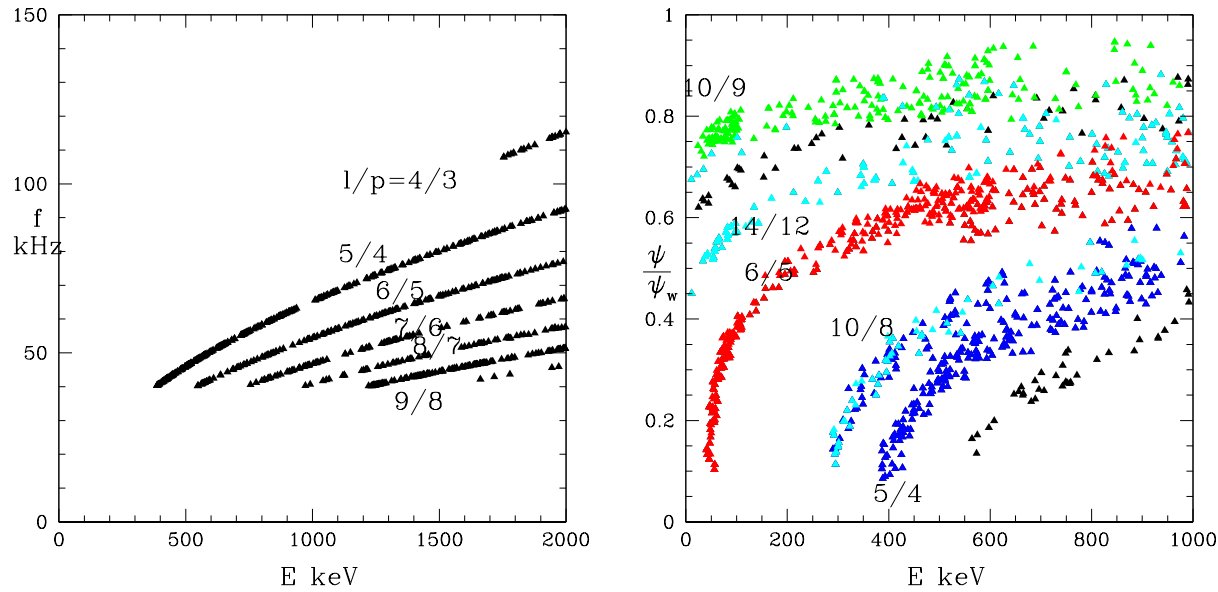
The equilibrium for W7X has a major radius of 550 cm and magnetic field of 24.7 kG.

The field has a toroidal period of 5

The q profile has a maximum of 1.2 near axis and falls to 1 at the edge.

Wide in minor radius, but very narrow in q .

Energy dependance of W7X negative frequency resonances



Negative frequency resonances in W7X vs particle energy with $-10 < l < -4$

The orbits have helicities slightly above the values of q on axis.

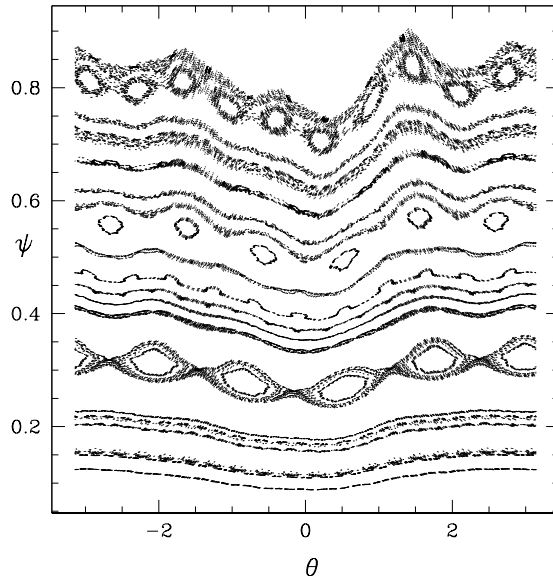
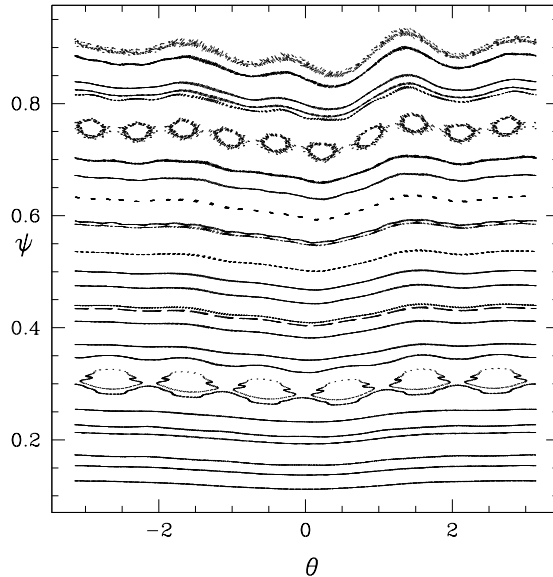
The $10/9$ resonance is present at very low energy

At about 50 keV the $6/5$ resonance enters with equilibrium period, arriving at the plasma center by 400 keV,

followed by the $10/8$ and $5/4$ resonances at 300,400 keV.

Resonance frequency scales as $1/l$ and \sqrt{E} .

W7X Resonances at 100 and 600 keV



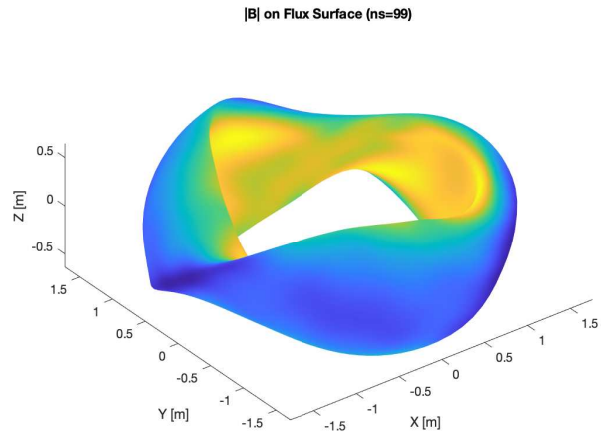
Poincaré sections of unperturbed counter moving particle orbits at 100 and 600 keV.

**Nonzero width with no eigenmode.
Resonance with toroidal field variation**

At 100 keV the 10/9 resonance has entered the plasma from the edge, and the 6/5 resonance has entered the plasma from the axis, but they produce very small resonance islands, and have very low frequencies, 10 and 17 kHz.

At 600 keV the 5/4 resonance has also entered from the axis and is at $\psi \simeq 0.3$ and the 6/5 resonance has moved to $\psi \simeq 0.6$.

NCSX

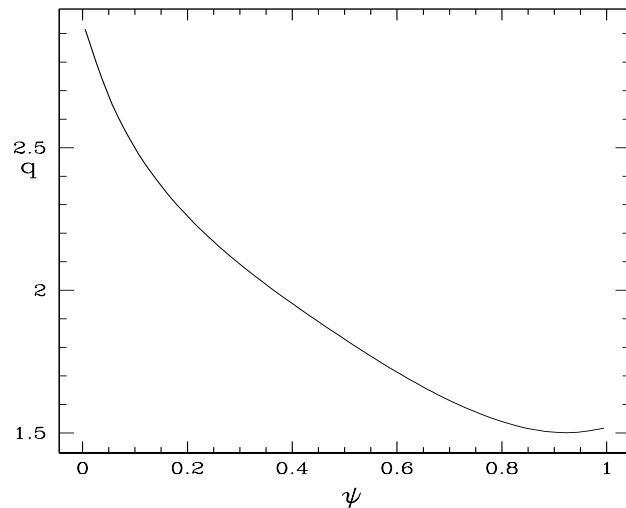


NCSX.

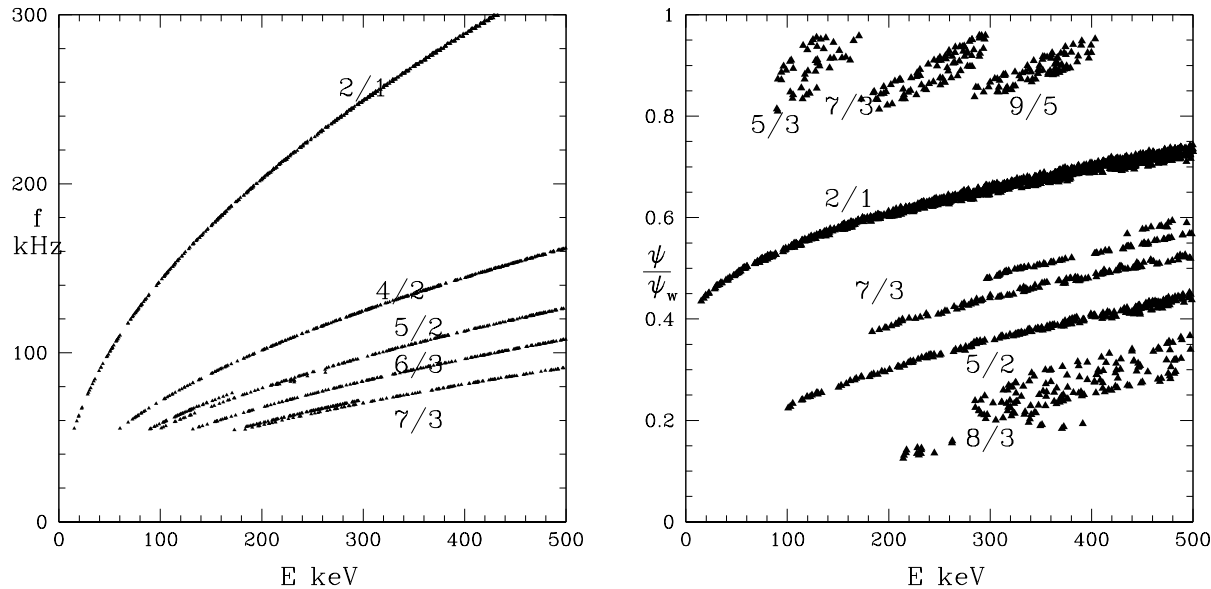
The equilibrium for NCSX has a major radius of 145 cm and magnetic field of 15 kG.

The field has a toroidal period of 3

The q profile has a maximum of 3. near axis and falls to 1.5 at the edge.



Energy dependance of NCSX negative frequency resonances



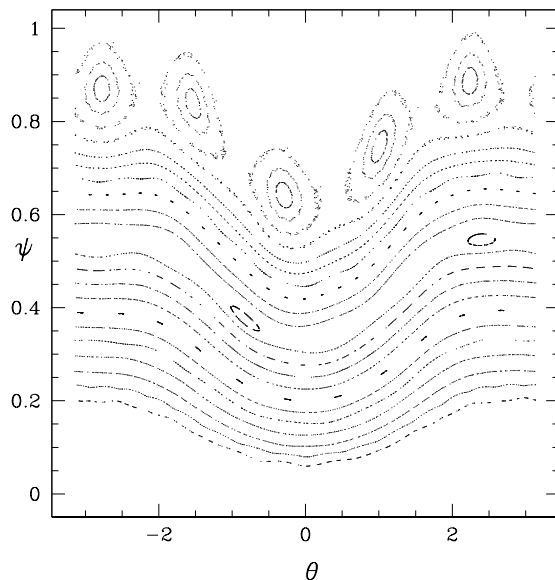
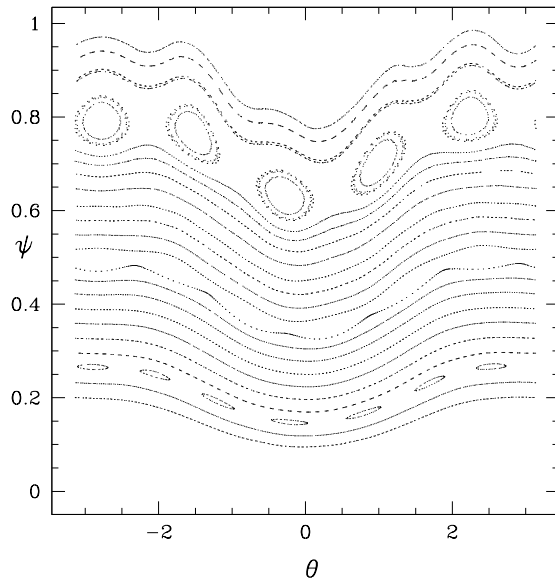
Negative frequency resonances in NCSX vs particle energy with $-5 \leq l \leq -2$

Helicities matching B are the $5/3$ and $7/3$ resonances

At low energy many resonances are present.

Resonance frequency scales as $1/l$ and the square root of the energy.

NCSX Resonances at 50 and 100 keV



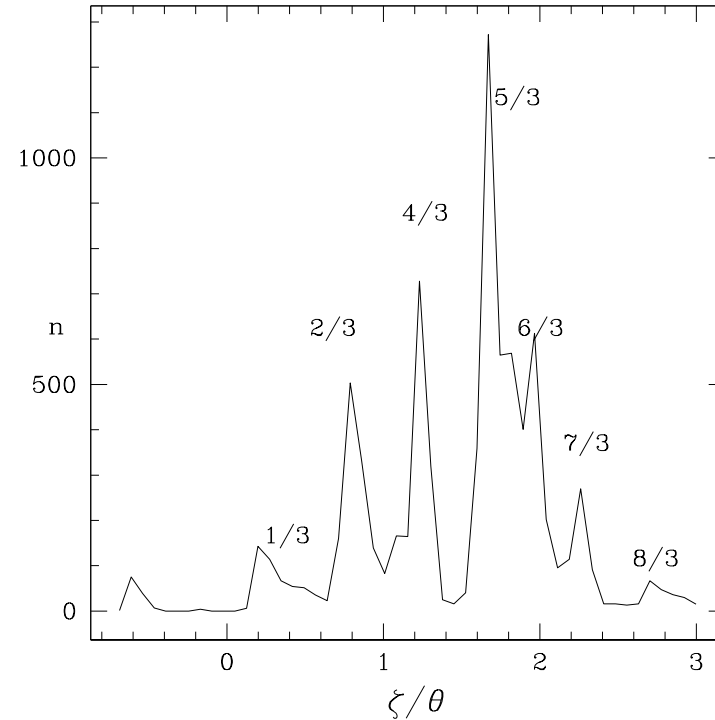
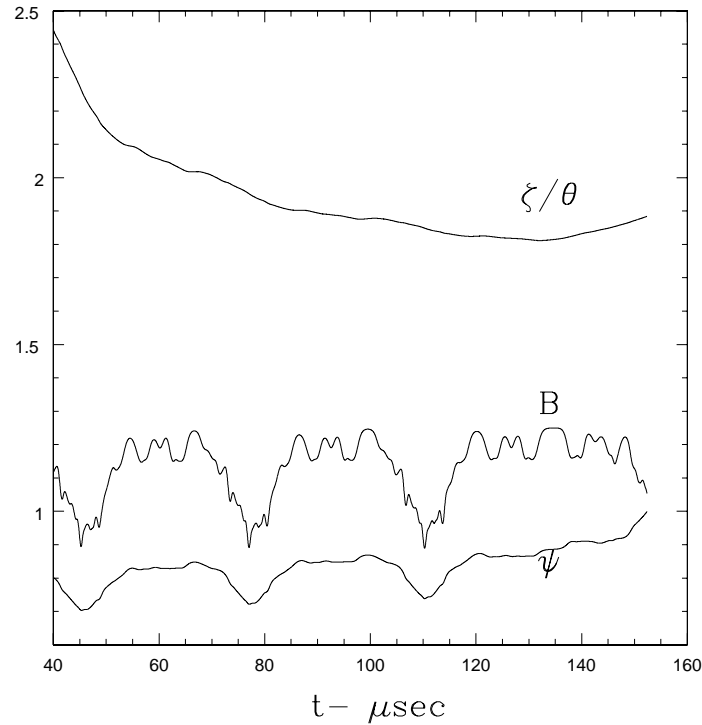
Poincaré sections of unperturbed counter moving particle orbits at 50 and 100 keV.
Nonzero width with no eigenmode.
Resonance with toroidal field variation
Equilibrium has toroidal period 3

At 50 and 100 keV the 5/3 resonance at $\psi = 0.9$ and the the 7/3 resonance at $\psi \simeq 0.3$ are visible

These are standing waves locked onto the equilibrium

The 5/3 and 7/3 resonate with the period 3 of B

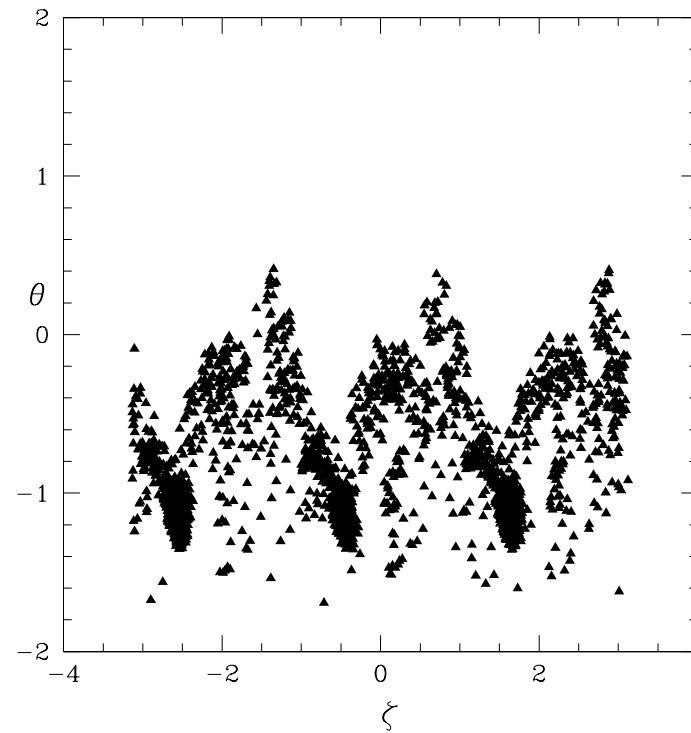
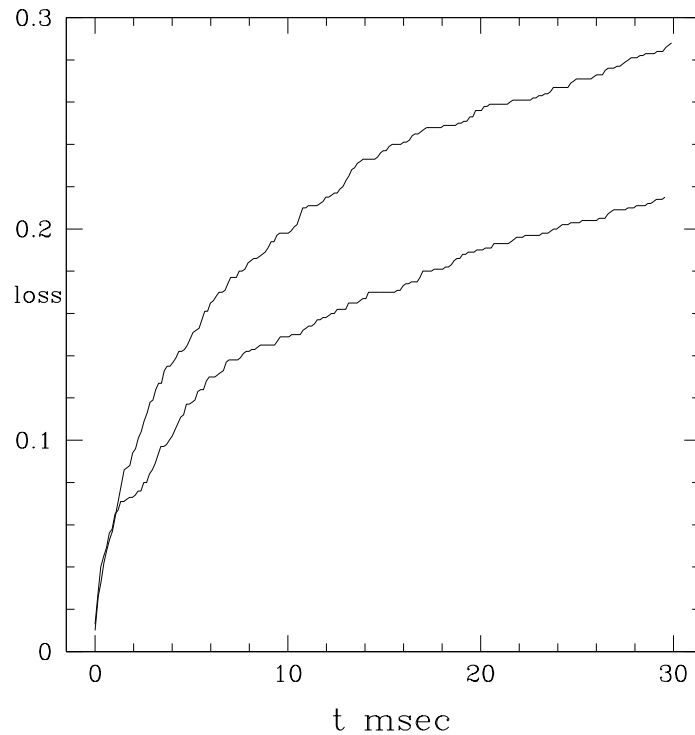
NCSX Ripple Trapping Alpha Loss



A typical loss trajectory in 10 meter NCSX. Shown is the value of ζ/θ , B and ψ along the orbit. The trace of B shows multiple attempts of trapping near $B = 1.2$.

Finally at 120 microseconds trapping long enough to produce loss occurs. Losses at resonances with toroidal period 3.

NCSX Ripple Trapping Alpha Loss

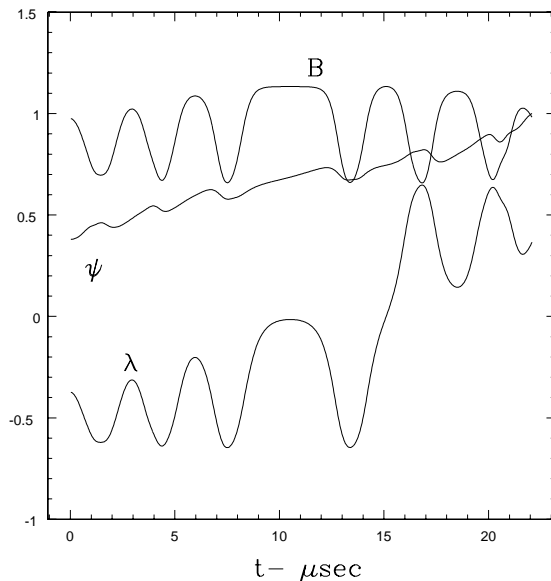
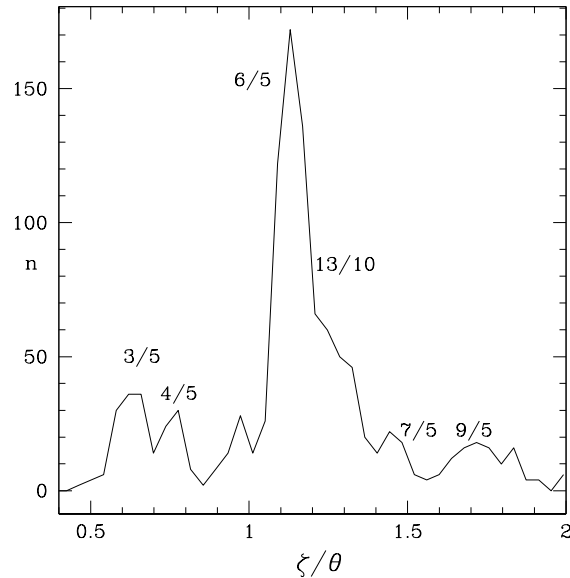


A 10 meter NCSX, with no collisions (lower) and with pitch angle scattering with collision time of 300 msec (higher).

Unacceptable losses in a short time, associated with equilibrium resonance induced ripple traps in the trajectories

Loss distribution shows the period 3 of the equilibrium

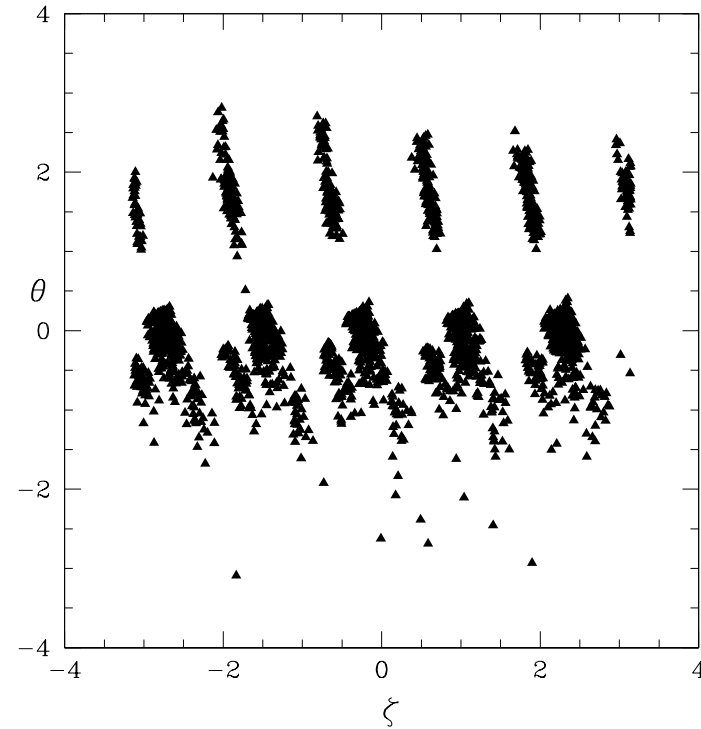
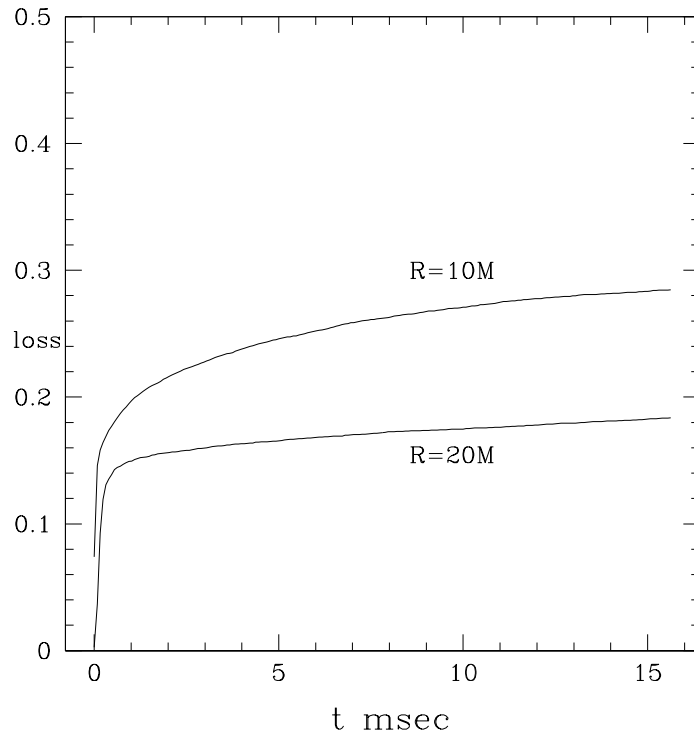
W7X Ripple Trapping Alpha Loss



Resonance islands produce local wells in orbits which give ripple trapping. Helicity distribution of lost alpha particle orbits on a ten meter five Tesla W7X.

Particles with helicity matching the toroidal helicity of the equilibrium are lost. Only the $6/5$ is strong enough to show clearly as an island in the Poincaré plot. A loss trajectory in the 10 meter W7X. Shown are B , ψ and pitch $\lambda = v_{\parallel}/v$ along the orbit. The particle is initially trapped in a resonance well and exits from deep in the plasma.

W7X Ripple Trapping Alpha Loss



Alpha particle loss versus time for 10 and 20 meter reactor W7X with no pitch angle scattering.

Alpha loss distribution showing the period 5 of the equilibrium

Orbital Chaos

Alfvén mode in a Stellarator without a symmetry

Time step depends on the value of ζ through $B(\psi, \theta, \zeta)$

A Poincaré frame ψ, θ is at times $n\zeta - \omega t = 2\pi k$

$$\dot{\psi} = mgB(\psi, \theta, \zeta)v_{\parallel}\alpha(\psi)\cos(\Omega), \quad \dot{\rho}_{\parallel} = v_{\parallel}^2\partial_{\psi}B(\psi, \theta, \zeta)\xi(\psi)\sin(\Omega).$$

for fixed ψ, θ with $\Omega = n\zeta - m\theta - \omega t$.

ζ is given by ωt so there is a random step in ψ and in ρ_{\parallel} given by

$$\dot{\psi} = m\delta(B)v_{\parallel}\alpha(\psi), \quad \dot{\rho}_{\parallel} = v_{\parallel}^2\delta(\partial_{\psi}B)\xi(\psi)$$

with δX equal to X minus the mean value of X over ζ .

This gives diffusion $\langle \psi^2 \rangle = Dt/2$ with $D = [mg\delta(B)v_{\parallel}\alpha(\psi)/2q]^2 dt$
and $[\delta(\partial_{\psi}B)v_{\parallel}^2\xi(\psi)/2q]^2 dt$ for ρ_{\parallel}

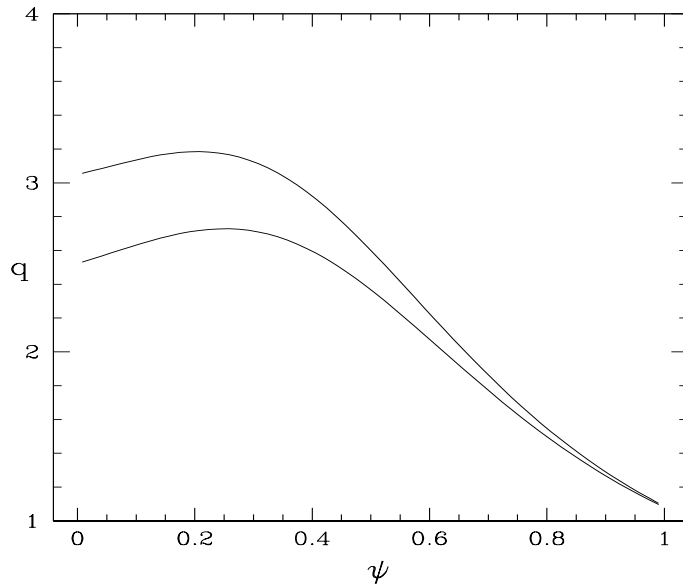
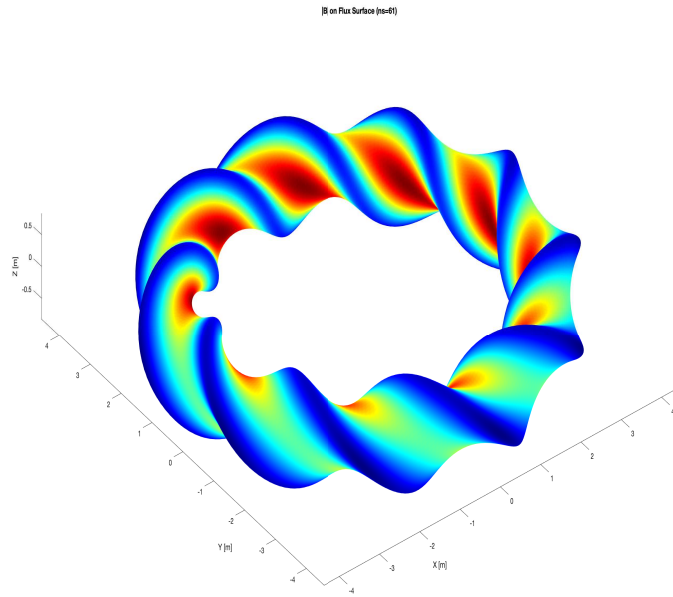
There is thus a strong effect of a small Alfvén mode
because the step is independent of energy and pitch.

Requirement of small $\partial_{\psi}B$ less strong, term second order in ρ .

Resonant Mode Growth

- High frequency Alfvén modes cause particle redistribution and loss.
- Modes can only be destabilized where there is a resonance.
- Mode growth and saturation depend on local gradients and damping.
- If a high frequency resonance exists there is high probability that a distribution of high energy particles will destabilize a mode at this location.
- Resonances can occur for co-moving or counter-moving orbits. They are very different because of drifts. Must examine both cases.
- In a symmetric device the distribution is modified in a local coherent manner due to rotation about resonance elliptic points
- In a nonsymmetric device the distribution change is chaotic and widespread, with immediate loss and large diffusion.

LHD



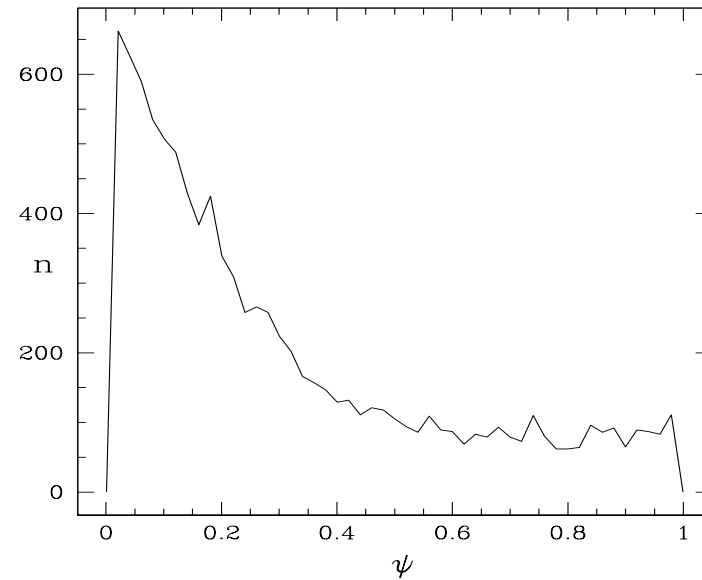
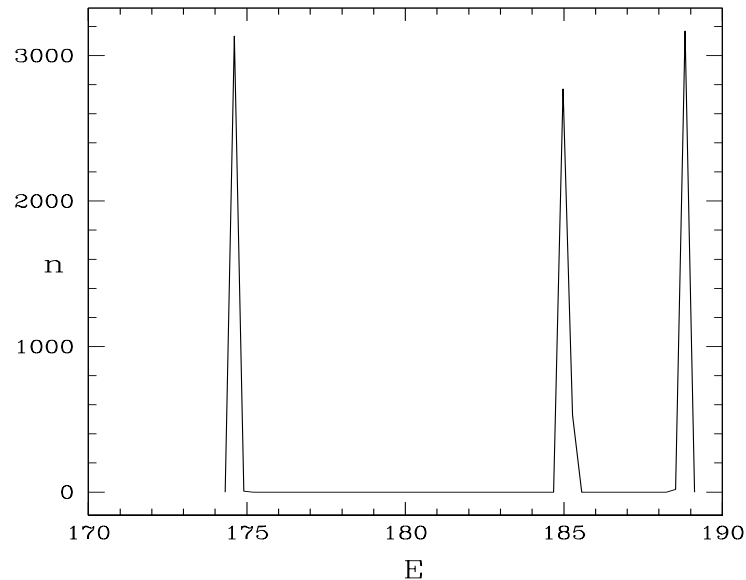
The Large Helical Device (LHD) is a fusion research device in Toki, Gifu, Japan

The LHD employs a heliotron field with toroidal period 10.

Typical q profiles during operation.

Examine Hydrogen beam discharge of 2010 and Deuterium beam discharge of 2022

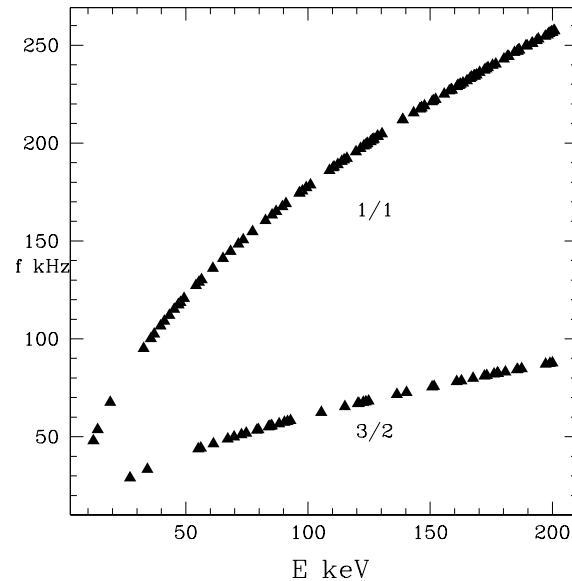
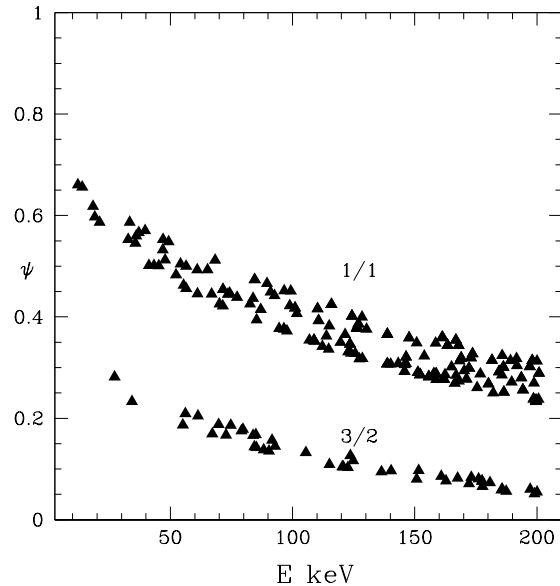
LHD 2010



Energy and deposition location ψ of the particles injected by the three Hydrogen beams during the 2010 experiment.

Two beams were counter passing, only the beam at 185 keV was co-passing.

LHD 2010



Resonances for the hydrogen beam discharge of 2010 showing location and frequency vs particle energy.

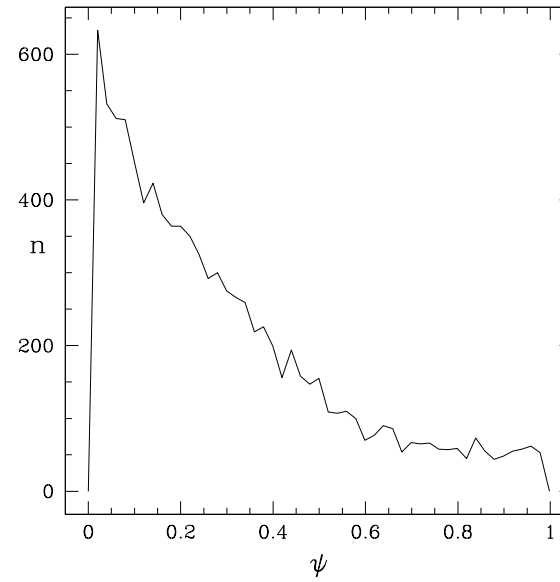
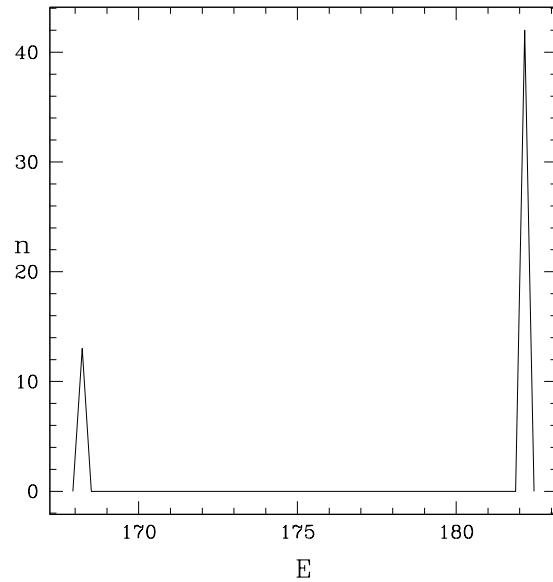
These resonances exist for deeply counter passing ions.

Frequency somewhat lower for smaller pitch.

Two of the three beams were counter and deeply passing.

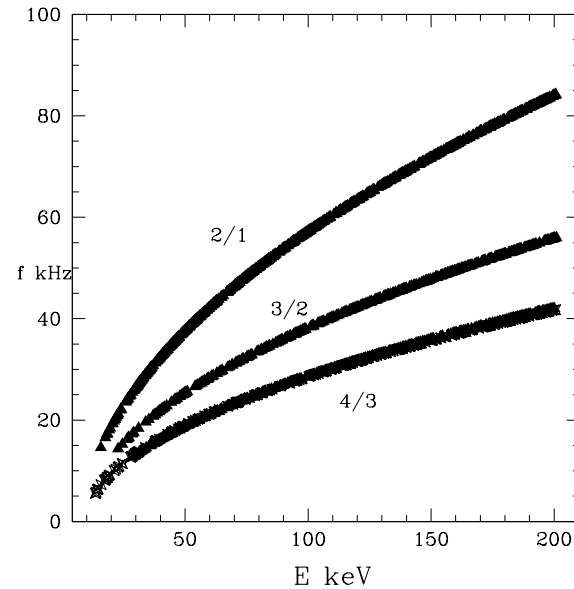
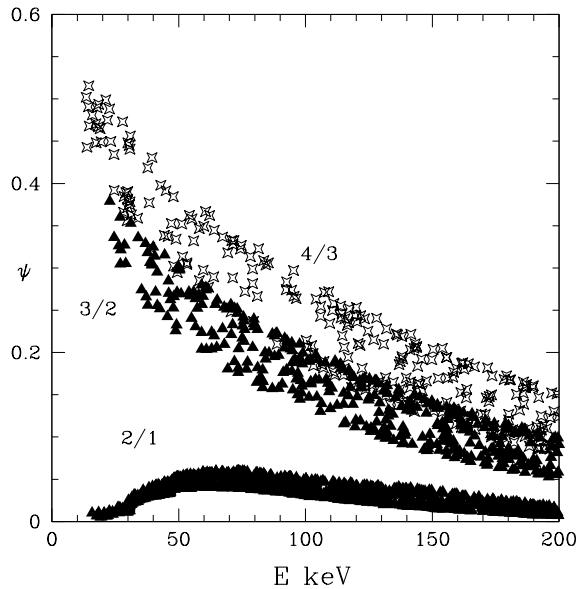
Experimentally observed and numerically found (1/1) Alfvén instability at 70 kHz causing particle loss.

LHD 2022



Energy and deposition location ψ of the Deuterium particles injected by the two beams during the 2022 experiment. The high energy beam was deeply co-passing, the low energy beam counter.

LHD 2022



Resonances for the deuterium beam discharge of 2022 showing location and frequency vs particle energy.

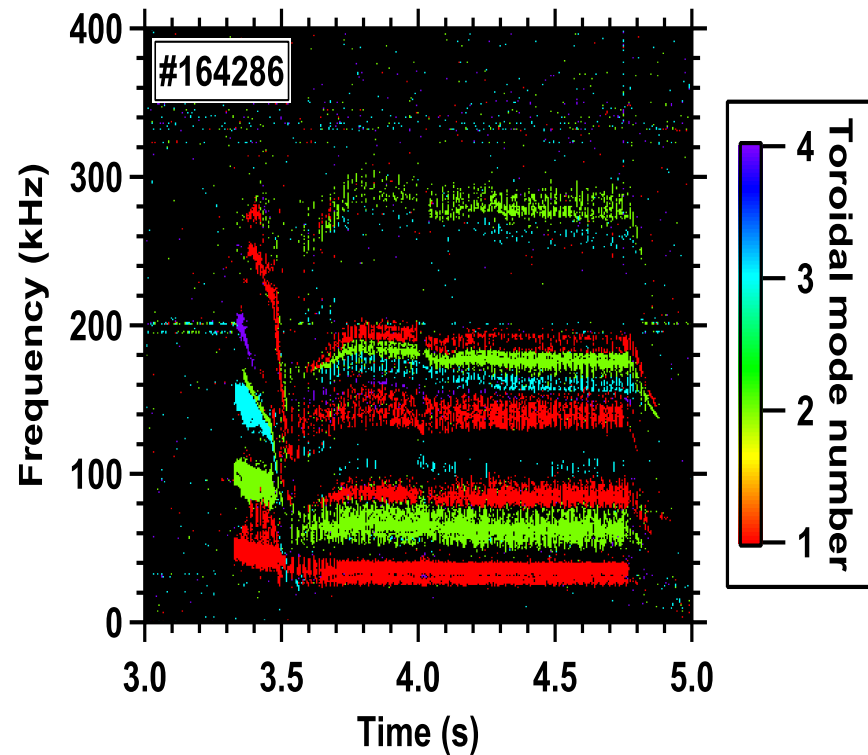
These resonances exist for deeply co-passing ions.

Equilibrium toroidal period is ten

Experimentally observed 40 kHz avalanche with particle loss, modes not identified but included $n = 1$ and probably also 3/2 and 4/3.

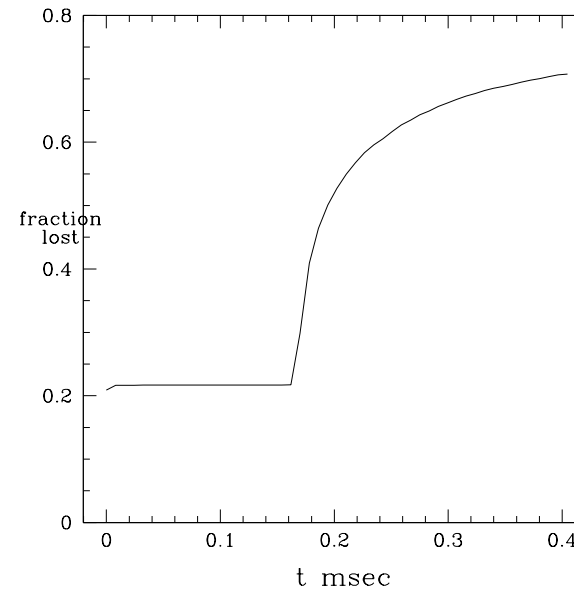
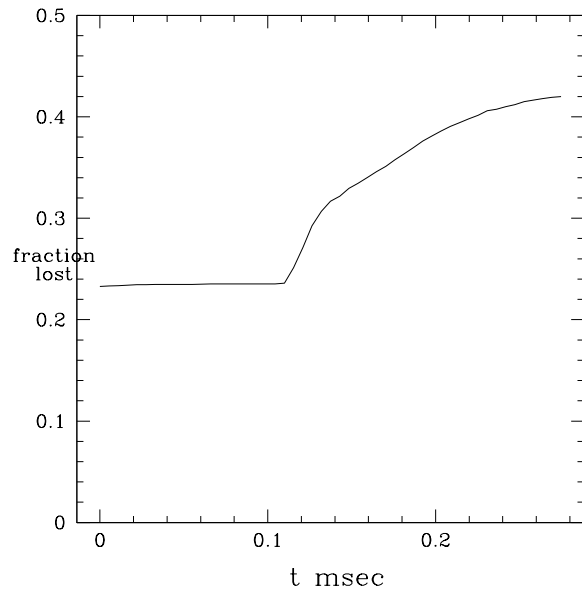
Conclude that the presence of a low mode number resonance and high energy particles will very likely destabilize an Alfvén mode.

LHD observed modes 2022



Determination
of modes in LHD 2022
An avalanche
was observed
with significant
particle loss

LHD



Simulated particle loss vs time for the discharges in 2010 and 2022

The mode delayed to distinguish prompt beam loss from TAE loss.

Prompt loss much larger in the first experiment with lower field.

TAE induced loss with mode amplitude of 10^{-6}

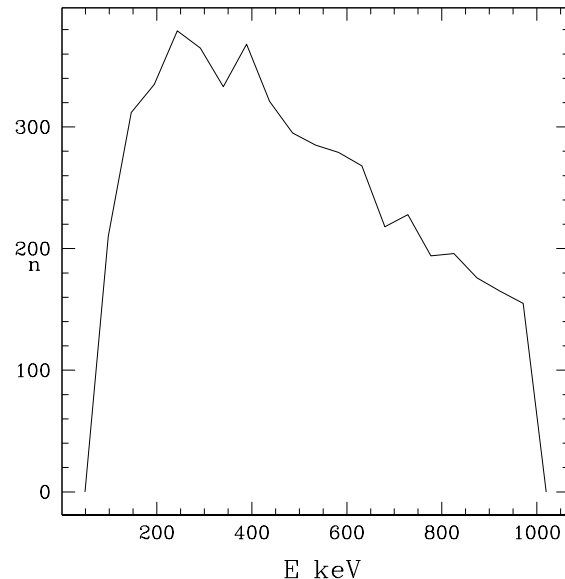
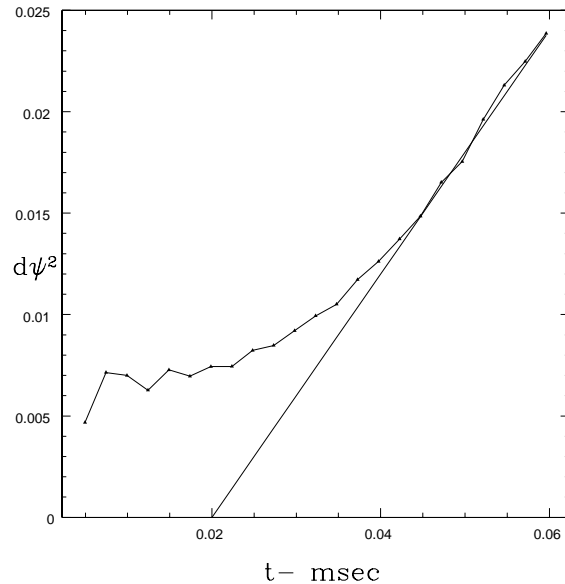
rises to about 40 percent of the initial beam.

Actual loss would depend on mode history,

flattening of local gradients and damping.

Large loss observed in experiments.

Chaotic diffusion in W7X with small Alfvén mode



$$\dot{\psi} = mg\delta B(\psi, \theta, \zeta)v_{\parallel}\alpha(\psi)\cos(\Omega),$$

with δX equal to X minus the mean value of X over ζ .

Mode induced loss in W7X due to a 70 kHz Alfvén mode with $m/n = 5/4$, with a uniform particle distribution in energy and flux, $A = 3 \times 10^{-8}$.

Diffusion in ψ

and energy of lost particles.

Particles passing through the domain where the amplitude is large are scattered into loss orbits, independent of energy or pitch.

Conclusion

- Initially an equilibrium can be chosen so that there are no low order rationals in the field line helicity $q(\psi)$, so no resonances.
- As particle energy increases resonances can emerge from the magnetic axis or the plasma edge, and move into the plasma.
- If the equilibrium has significant toroidal variation and resonances match the toroidal B , islands form even with no unstable mode, width increasing with particle energy. Trapped orbits in these resonance give strong ripple trapping loss.
- Alfvén modes are easily destabilized at resonances.
- If the equilibrium is not symmetric a mode produces chaotic diffusion and loss of all energies and pitch at small mode amplitude.
- Following LHD results we conjecture that Alfvén modes will always appear where there is a high frequency resonance.
- Avoiding resonance islands must become a part of stellarator design. Symmetrization requirement is severe